Ontogenetic stages of ceratopsian dinosaur *Psittacosaurus* in bone histology

QI ZHAO, MICHAEL J. BENTON, SHOJI HAYASHI, and XING XU

Zhao, Q., Benton, M.J., Hayashi, S., and Xu, X. 2019. Ontogenetic stages of ceratopsian dinosaur *Psittacosaurus* in bone histology. *Acta Palaeontologica Polonica* 64 (2): 323–334.

The early ceratopsians *Psittacosaurus* and *Protoceratops* have provided important information on dinosaurian development because of abundant specimens of adults, subadults, juveniles, and even hatchlings. Here we present new data and methods for identifying key growth stages from bone histology. Previous studies on *Psittacosaurus lujiatunensis* from the Early Cretaceous Jehol Biota of China did not present in-depth analysis of growth patterns. Based on a histological study of 43 thin sections from 17 individuals of this species, we recognize four histological ontogenetic stages, i.e., hatchling, juvenile, sub-adult, and adult, but no fully-grown stage. We estimate life history and longevity from diaphyseal growth line counts and other features of histology. We show that *P. lujiatunensis* grew fast in early stages (hatchling, juvenile, and subadult), according to the density of vascular canals and the different type of bone tissue; the deposition of parallel fibred bone tissue in the outer cortex of the subadult stage indicates that growth rate was slowing down. We introduce a new graphical method to estimate the occurrence and volumes of vascular canals from thin sections more accurately than current two-dimensional approaches.

Key words: Dinosauria, Ceratopsia, bone histology, ontogeny, growth patterns, longevity, Cretaceous, China.

Qi Zhao [zhaoqi@ivpp.ac.cn] and Xing Xu [xu.xing@ivpp.ac.cn], Key Laboratory of Vertebrate Evolution and Human Origins, Institute of Vertebrate Paleontology and Paleoanthropology; and Center for Excellence in Life and Paleoenvironment, Chinese Academy of Sciences, Beijing 100044, China.
Michael J. Benton [Mike.Benton@bristol.ac.uk], School of Earth Sciences, University of Bristol, Bristol BS8 1RJ, UK.
Shoji Hayashi [hayashi@big.ous.ac.jp], Department of Biosphere-Geosphere Science, Okayama University of Science, Okayama, 700-0005, Japan.

Received 18 October 2018, accepted 29 January 2019, available online 4 March 2019.

Copyright © 2019 Q. Zhao et al. This is an open-access article distributed under the terms of the Creative Commons Attribution License (for details please see http://creativecommons.org/licenses/by/4.0/), which permits unrestricted use, distribution, and reproduction in any medium, provided the original author and source are credited.

Introduction

Several studies on dinosaurs (e.g., Erickson and Tumanova 2000; Horner et al. 2000; Klein and Sander 2008; Klein et al. 2009) have demonstrated that histological sections of fossil bone samples can be used to establish the relative age/ontogenetic stage of specimens. The bones of prematurely dead young dinosaurs may well record their ontogenetic history, as shown by Woodward et al. (2014) in alligators, and by Woodward et al. (2015) in *Maiasaura*. However, this is generally not the case with bones of older individuals, because remodelling during growth can remove any number of growth rings in the centre of the bone. In such cases, it is necessary to look at more than one bone, and instead a series of bones from individuals of the same species, whose age can be estimated, can provide overlapping histological records of younger and older individuals to elucidate the full ontogenetic growth trajectory for the species (Zhao et al. 2013). There are many *Psittacosaurus* skeletons, including juveniles to adults, in the Institute of Vertebrate Paleontology and Paleoanthropology (Beijing, China), showing various ontogenetic stages. These provide a unique opportunity to explore character changes through ontogeny and establish the life history and growth pattern for *Psittacosaurus lujiatunensis*.

The key assumption behind establishing the age of reptiles and mammals by skeletochronology is that the region between the two neighbouring LAGs (lines of arrested growth) represents one year of growth, with the LAG indicating a temporary cessation of growth in winter or another unfavourable season (Francillon-Vieillot et al. 1990; Ricqlès et al. 1991; Castanet et al. 1993; Sander and Klein 2005; Köhler et al. 2012). The LAG is marked by a darker band in thin section, representing the increased density of the bone as a result of less bone deposition and fewer canals formed within a fixed amount of time.

Using this approach, Erickson and colleagues sought to reconstruct life tables and assumed logistic growth curves for a variety of dinosaurs, such as *Tyrannosaurus*,

Oviraptor, and *Psittacosaurus* (Erickson and Tumanova 2000; Erickson et al. 2001, 2004, 2006, 2007, 2009; Erickson 2005;). The methods have attracted a great deal of attention, even though they have been criticised by Sander et al. (2004) because some dinosaurs such as sauropods grew very fast and show limited data on their earlier years in bone sections. New work on large mammals (Köhler et al. 2012) has shown that older assumptions that LAGs are associated only with ectothermic physiologies are incorrect. Modern ruminant mammals also show evidence of cyclical growth. Growth slows or stops during the unfavourable season, associated with reductions in body temperature, metabolic rate, and suppression of bone growth regulators. The occurrence of dry seasons, for example, can drive patterns where, for example, there might be two episodes of starvation in a year and hence two LAGs (Castanet 2006).

We assume that the use of LAGs to indicate age is most reliable when juveniles and adults are sampled from the same locality, which means that the individual animals all experienced similar climate cycles. By superimposing the drawing of LAGs and determining numbers of LAGs, age at death can be determined for *Psittacosaurus*, using methods and data presented by Zhao et al. (2013).

Previous work on the bone histology of *Psittacosaurus* includes a detailed study of ontogenetic stages in *P. mongoliensis* by Erickson and Tumanova (2000) and a similar study on *P. lujiatunensis* by Erickson et al. (2009). In our earlier work (Zhao et al. 2013), we addressed questions of age estimates and evidence for differential bone growth rates related to a postural shift from quadrupedal juveniles to bipedal adults.

In this study, we describe the histological ontogenetic changes in *Psittacosaurus lujiatunensis* in further detail and compare these with the previous histological work on *P. mongoliensis*. Our aim is to explore the bone histology of each growth stage of *P. lujiatunensis*, in particular presenting the changes in histological tissue types as shown by confidently aged individuals. We report that the growth pattern in bone histology is different between these two species, and we develop this theme further as an example to show the complexity of growth patterns in dinosaurs.

Institutional abbreviations.— ELDM, Erlianhaote Dinosaur Museum, Eerenhot, Inner Mongolia, China; IVPP, Institute of Vertebrate Paleontology and Paleoanthropology, Beijing, China.

Other abbreviations.—EFS, External Fundamental System; LAG, line of arrested growth.

Material and methods

Material and age estimation.—In this study, 17 individuals of *Psittacosaurus lujiatunensis* from the Early Cretaceous Jehol Biota of China were histologically sampled, resulting in 43 thin sections taken from the midshafts of humeri, ulnae, radii, femora, tibiae, and fibulae (Table 1). The sample spans a growth series from hatchling to adult developmental stages, determined according to life history and longevity estimates based on diaphyseal growth line counts, the growth stages of osteons and other features of histology, as explained by Zhao et al. (2013). The broad assumption, as in other studies of dinosaurs, is that the LAGs represent approximate annual growth indicators.

Table 1. Numbers of LAGs in individual thin sections made during this study. Values in parentheses represent additional LAGs that are inferred to have been obliterated by expansion of the medullary cavity. An age estimate is given for each specimen, based on the evidence from all thin sections taken for that specimen. For IVPP V12617, the cross-section through the radius suggests a younger age (seven years) than cross-sections through the other sampled bones (ten years). However, only one juvenile radius was sectioned in this study, and it is possible that we have underestimated the number of LAGs obliterated by medullary cavity expansion in the radius of IVPP V12617.

Repository number	Humerus	Ulna	Radius	Femur	Tibia	Fibula	Age
IVPP V16902.1				0	0		<1
IVPP V16902.2	0			0			<1
IVPP V16902.3					0		<1
ELDM V1037					1		1
ELDM V1038.21	2	2		2	2		2
ELDM V1038.15					2	2	2
ELDM V1038.11	2	2		2	2	2	2
IVPP V14341.2					2	2	2
IVPP V14341.3					2	2	2
IVPP V14341.4					2	2	2
IVPP V14341.5					2	2	2
IVPP V14341.6	2	2	2				2
IVPP V14341.1	3			3	2 (1)	3	3
IVPP V14748					3 (2)	3 (2)	5
IVPP V18344			4 (2)	3 (3)	5 (2)	6 (1)	7
IVPP V18343	5 (3)					8 (1)	9
IVPP V12617	7 (3)		5 (2)		8 (2)		10

We were inclined to accept this simple correlation of LAG numbers and age as reasonably accurate, for younger individuals at least, as multiple juveniles from a single clutch of six specimens (IVPP V14341) showed comparable patterns of LAGs, five of them being two years old, and one slightly larger individual three years old (Zhao et al. 2013). In older individuals, we explored geometric ways to detect whether early LAGs had been resorbed by medullary cavities. For example, we took thin sections of the humerus, femur, tibia, and fibula from the largest of six individuals of *Psittacosaurus lujiatunensis* (IVPP V14341.1). Following different rates of medullary cavity expansion in each bone, we found three LAGs in the humerus, femur, and fibula, but just two LAGs in the tibia. The medullary cavity must have absorbed the first-year LAG in the tibia. To test this, we took a further eight tibial and fibular thin sections in different individuals of the same cluster (IVPP V14341.2, IVPP V14341.3, IVPP V14341.4, IVPP V14341.5). There

are just two LAGs in each thin section. We drew each LAG on paper under the microscope, and then overlapped the images. We found that the medullary cavity of the tibia of IVPP V14341.1 is much larger than the others, and its size overlaps the first-year LAG in the other tibiae. This suggests that the first LAG had indeed been resorbed during growth.

Creation of thin sections.—Histological thin sections of long bones were made using standard techniques by cutting and grinding for hard tissue histology (Sander 2000; An and Martin 2003). Previous studies of dinosaur long-bone histology, as well as general principles of bone growth, indicate that a section taken at the middle of the shaft of a long bone is generally optimal for obtaining a maximally complete growth record from that bone (Erickson and Tumanova 2000; Horner et al. 2000; Sander 2000). This arises from the predominantly appositional growth of this part of the shaft, and the location of the neutral zone in this region (Sander 2000).

Specimens were embedded in resin, and mid-shaft diaphyseal transverse thin-sections were cut using a diamond circular saw fitted with a diamond-tipped wafering blade. One surface of each section was smoothed with a wheel grinder/polisher, and then ground manually using grinding powder (600 grit) to produce a smooth texture ideal for gluing to a glass slide. The section was then cut to a thickness of about 250 μm with a diamond circular saw before being ground further to the desired final thickness of 50–80 μm, leaving the exposed surface of the section smooth. Each slide was then cleaned in a water-filled ultrasonic cleaner to remove microscopic grit, and finally capped with a glass coverslip. The completed thin sections were studied in normal and polarized light.

Throughout the text, we use standard bone histological terminology and definitions, as in Francillon-Vieillot et al. (1990), Horner et al. (1999), Erickson (2005), and Klein and Sander (2008).

Interpreting vascular canal types.—A problem with earlier work in bone histology is that vascular canals are generally viewed in two dimensions. This is because, of necessity, researchers work with standard petrological-type thin sections that they inspect under the microscope. More often, they work from micro-photographs, and simply mark on the vascular canals as differences in colour between bone and canal fill. The margins are usually sharp, and it might be assumed that a two-dimensional view could be sufficient for identification of canal type, and estimation of the relative abundances of each kind of vascular canal (longitudinal, reticular, radial, circular) and volumes of osteocyte lacunae.

In fact, we found in our study that this standard approach can be quite misleading. Chance cuts through radial or longitudinal canals at an angle, showing only a circular or elliptical cross-section, can make them look as if they are longitudinal canals. Even though the slides are the standard thickness of 50–80 μm, this is enough to observe change along the z-axis of canals that are themselves 10–40 μm across; what starts as a simple circular cut orthogonal to the axis of a canal at the top of the slide can show branching within the slide thickness, and cause a reinterpretation of the canal type, for example. Reticular canals can be missed entirely. An attempt should be made to view the sections in three dimensions, as described below, especially if the types of vascular canals are used to indicate growth rates.

Here, we adopted a new graphical approach, which, while more time-consuming than regular approaches, gives, we believe, a much more accurate identification of the categories and density of vascular canals. The first basic step is to view the bone thin sections under normal light and polarised light. Second, we then focus the microscope stage up and down and follow individual canals through the depth of the thin section. In certain cases, for example, what looked like longitudinal canals on the surface of the slide turned out to be reticular as we focused up and down (see SOM: figs. S1–4, Supplementary Online Material available at http://app.pan.pl/SOM/app64-Zhao_etal_SOM.pdf).

Our racking up and down graphical method is analogous to the image-stacking technique in microphotography, a widely-used method in palaeontology (e.g., Kerp and Bomfleur 2011; Selden and Penney 2017) and other fields, but we did not use this approach, to make deep-view photographs because our purpose is to use the information analytically. This requires the production of diagrams that code the canal types accurately and to scale so that statistical analysis may be done. For the diagrams, we use a standard set of colours, namely, longitudinal vascular canals (navy), reticular vascular canals (green), radial vascular canals (red), circular vascular canals (sky blue) and LAGs (brown lines). Examples of figures showing this approach are Figs. $2A_3$, $3A_3$, $4A_3$–C_3, $6A_3$–D_3, $8A_3$, C_3, D_3, F_3. These colour-coded diagrams provide a more immediate analysis of the canal types than digital outputs of image-stacked photographs, and they enable statistical counts of numbers and density of different canal types.

We measured density of canals using the measuring tools on the Zeiss PrimoTech microscope. The magnification was set to 20×, and the field of view represented 0.572×0.429 mm. This is an area of 0.245 mm^2, and we converted the counts to counts per mm^2 by multiplying by 4.1. We tagged canals of different types and the operating software generated tables of density of canals (number of canals within field of view), as well as canal measurements (maximum and minimum diameters).

Results

Based on the new approach of observing vascular canals and the histological information in the series of thin sections from *P. lujiatunensis*, we recognize four histological ontogenetic stages, i.e., hatchling, juvenile, sub-adult, and adult. None of the specimens was fully-grown (Table 2). The main description of the bone histological information is based on the tibia in each stage, because the tibia is the only bone

Fig. 1. The cluster of hatchling ceratopsian dinosaur *Psittacosaurus lujiatunensis* Zhou, Gao, Fox, and Chen, 2006 (IVPP V16902) from western Liaoning, China, Early Cretaceous.

represented at each growth stage. Comparisons between different limb bones in each stage are also demonstrated.

Hatchling stage.—According to the histological characters, the specimen IVPP V16902, a cluster of five hatchling individuals (Fig. 1), is considered as hatchling stage. These are also the smallest individuals that have been found. We made five sections from this cluster, including one humerus, two femora, and two tibiae.

In this ontogenetic stage, the vascular organisation in the tibia comprises mainly reticular vascular canals, although some simple longitudinal vascular canals are occasionally present (Fig. 2). Many reticular vascular canals look like longitudinal vascular canals in regular transmitted light (Fig. 2B$_1$, see SOM: fig. S1). Under polarised light, we can see these canals are actually reticular canals (Fig. 2B$_2$, B$_3$; see SOM: figs. S2, S3). This is proved by changing the focus under the microscope observation, which shows that the "longitudinal" canals are connected to each other in the deeper layer (see SOM: fig. S4). Some vascular canals are in radial rows (Fig. 2A). Incomplete periosteal vascular canals may be readily seen around the undulating periosteal surface (Fig. 2B). The density of the vascular canals and osteocyte lacunae is very high, with 188 per mm^2, with no difference from inner to outer cortex (see SOM: table S1).

Most vascular canals are simple primary vascular canals in this youngest stage, which shows no lamellar bone surrounding (Fig. 2C). Primary Haversian cavities, which have obvious large holes or cavities, are present close to the outer cortex. This is an early stage of fibrolamellar bone formation, showing the space that will later become infilled with lamellar bone tissue. A few primary osteons can be observed in the inner cortex, having a very thin layer of lamellar bone tissue around, but very few osteocyte lacunae embedded in the lamellar bone tissue (Fig. 2B; SOM: fig. S5). The margin of the simple primary vascular canals is irregular, similar to that of small erosion cavities in later ontogenetic stages. The diameter of vascular canals is larger than those observed in later ontogenetic stages (see SOM: tables S1–S4) as well as in very young stages of *Maiasaura peeblesorum* (Horner et al. 2000), *Phuwianosaurus, Apatosaurus* (Klein and Sander 2008), and oviraptorids (Wang et al. 2016). No secondary osteons are present. Most of the osteocyte lacunae are oval or nearly round in cross section (Fig. 2C), because most osteocytes are embodied in woven bone. A few elongate and flattened osteocyte lacunae tend to be arranged circumferentially close to the periosteal surface.

No LAG is present in any of the thin sections, indicating the individuals are all under one year old. The bone tissue is dominated by woven bone, with little lamellar bone around vascular canals. There is no parallel-fibred bone deposit in the outer cortex bone, and no erosion cavity around the medullary cavity.

Compared to the tibia, most of the bone histology information on the humerus and fibula is similar. The only difference with the tibia is the organisation of vascular canals which is dominated by longitudinal canals in the femur and represented equally by longitudinal and reticular canals in the humerus.

Juvenile stage.—We identified ten individuals from bone histological characters as juveniles (IVPP 14341, ELDM V1037, and ELDM V1038) and examined 27 thin sections from their humeri, ulnae, radii, femora, tibiae, and fibulae (Table 1).

Table 2. Bone microstructure in different ontogenetic stages of *Psittacosaurus lujiatunensis*.

	Hatchling	Juvenile	Sub-adult	Adult
Simple primary vascular canals	abundant	abundant	few	few
Longitudinal and circular primary osteons	no	few	abundant	few
Erosion cavity in inner cortex	no	no/few	few/abundant	abundant
Secondary osteons	no	no	yes	yes
Secondary remodelling	no	no	no	yes
Dominated bone tissue type	woven	fibrolamellar	fibrolamellar	fibrolamellar
Parallel-fibred bone in outer cortex	no	no	yes	yes
Endosteal bone	no	not completed	not completed	thick, completed
LAG erosion	no	no/yes	yes	yes
Vascularization reduced in outer cortex	no	no	slightly	obviously

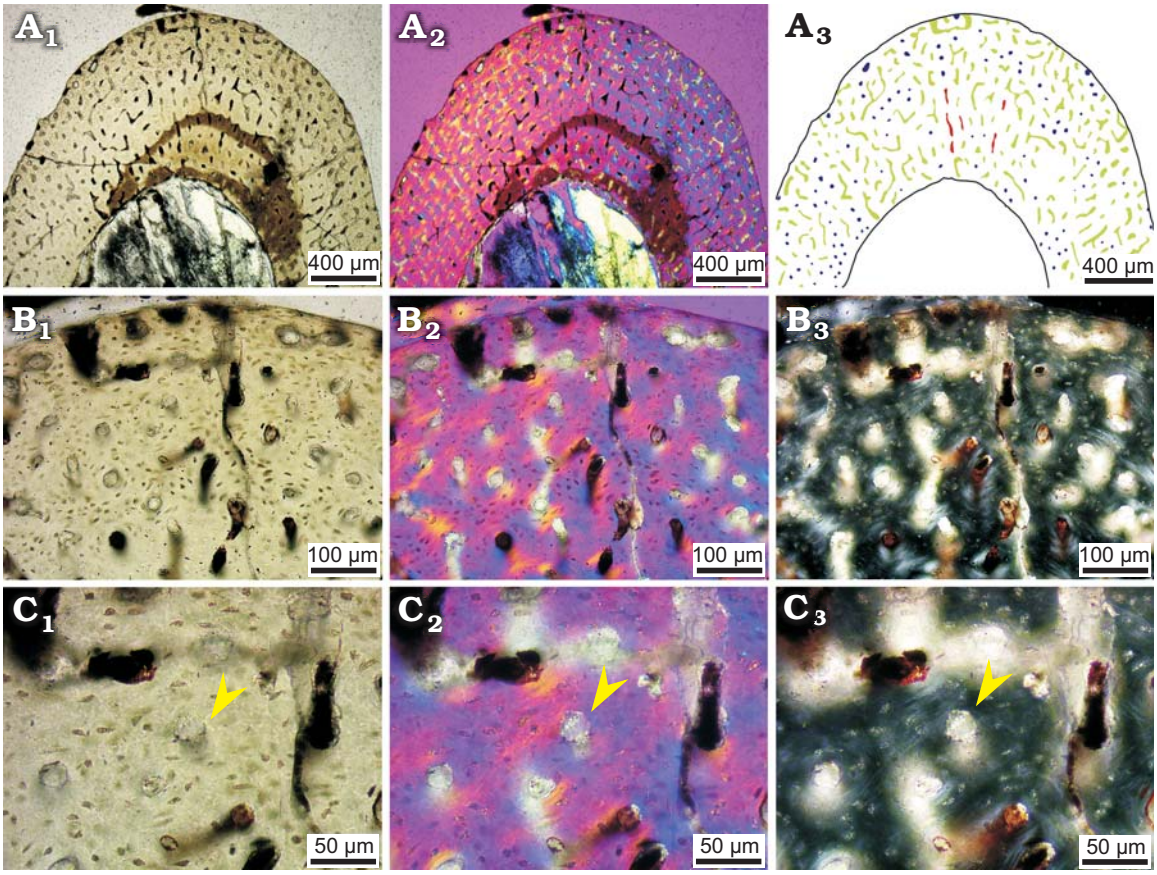

Fig. 2. Bone microstructure in hatchling ceratopsian dinosaur *Psittacosaurus lujiatunensis* Zhou, Gao, Fox, and Chen, 2006 (IVPP V16902.1) from western Liaoning, China, Early Cretaceous. **A**–**C**. Mid-diaphyseal transverse section of tibia (**A**) and details (**B**, **C**); photographs in regular transmitted light (A_1–C_1), elliptically polarized light (A_2–C_2), crossed plane-polarized light (B_3, C_3). A_3, line drawing showing longitudinal vascular canals (navy), reticular vascular canals (green) and radial vascular canals (red). Arrows indicate simple primary vascular canals.

Similar to the hatchling stage, the main vascular organisation in the tibia is also reticular vascularization, but longitudinal vascularization is also obvious (Fig. 3). The arrangement of vascular canals varies within bones in the same individuals; for example, radial vascular canals are obvious in some forelimb elements such as the humerus and radius (Fig. 4A, B). In the tibia, reticular vascular canals are more developed than in the hatchling stage. Longitudinal vascular canals in radial rows are also present in some parts of the bones, such as the humerus and radius (Fig. 4A, B). This feature seems to be accompanied by radial canals. A limited number of circular primary osteons are seen around the LAGs (Fig. $3A_1$)

Simple primary vascular canals are present close to the outer cortex (Fig. 3B). Different from the hatchling stage, the primary osteons in the inner cortex are developed, and here the osteocyte lacunae around the vascular canals are embedded in lamellar tissue (Fig. 3C). The margins of each simple primary vascular canals are distinct and round. The diameter of vascular canal has become short compared to the hatchling stage but is similar to that of later ontogenetic stages (see SOM: tables S2–S5). By comparing the numbers of vascular canals between inner cortex and outer cortex in each limb bone, we found the densities of vascular canals are still very high in the inner cortex, but decrease very slightly from the inner to outer cortex (SOM: table S6), from 44–57 (180–234 per mm^2) to 31–46 (127–189 per mm^2), the latter comparable to densities throughout the bone of the hatchling. All the osteons are primary osteons. Although most osteons just have one layer of osteocyte lacunae around them, some osteons in the inner cortex have two or three layers of osteocyte lacunae (Fig. 3C). Secondary osteons are still absent at this stage. The osteocyte lacunae are oval or nearly round in the inner cortex in cross section (Fig. 3C) but become more flattened in the outermost cortex (Fig. 3B).

LAGs are present circumferentially and cyclically in the cortex. There are lamellar bone tissue deposits around LAGs (Figs. $3A_2$, $4C_2$, C_3; see SOM: fig. S6), indicating a decrease in growth rate at particular periods every year. The main bone tissue is fibrolamellar bone, even in the outermost cortex (Fig. 3B). Endosteal bone is deposited partly around the medullary cavity in some limb bone elements, such as the ulna, radius, femur, and fibula, but it does not form a complete circle (Fig. 4D–G). Several erosion cavities are present close to the endosteal bone in the femur and fibula (Fig. 4F, G). The outline of the medullary cavity is not smooth, and the shape varies in different bones (Fig. 4D–G).

Sharpey's fibres are present in the middle and outer cortex of the tibia where it is close to, but not connected to the

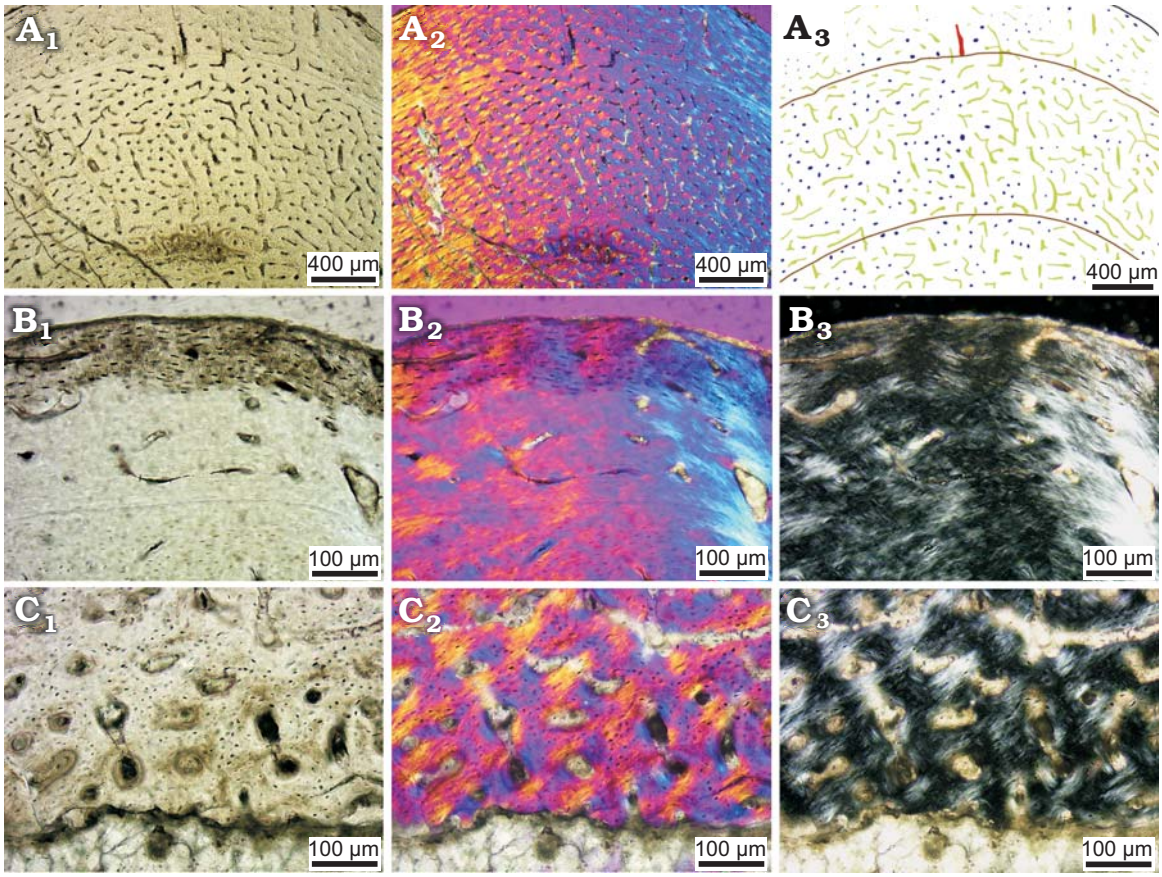

Fig. 3. Bone microstructure in juvenile ceratopsian dinosaur *Psittacosaurus lujiatunensis* Zhou, Gao, Fox, and Chen, 2006 (IVPP V14341.1) from western Liaoning, China, Early Cretaceous. **A**–**C**. Mid-diaphyseal transverse section of right tibia (**A**), the outer most cortex (**B**), the inner most cortex (**C**); photographs in regular transmitted light (A_1–C_1), elliptically polarized light (A_2–C_2), crossed plane-polarized light (B_3, C_3); line drawing (A_3) showing longitudinal vascular canals (navy), reticular vascular canals (green), radial vascular canals (red), and LAGs (brown lines).

fibula (Fig. 4H_1, H_2), indicating a soft tissue connection between these bones.

Sub-adult stage.—We identified two individuals as the sub-adult stage based on bone histological characters (IVPP V14748 and IVPP V18344; Fig. 5) of six transverse thin sections from one radius, one femur, two tibiae, and two fibulae.

The main organization of vascular canals varies in different bones. In the radius, femur, and tibia, reticular vascular canals are the dominant type of vascular canals, which is quite different from the juvenile stage (Fig. 6A–C). Slightly different from other bones, the reticular vascular canals show more complex network in femora (Fig. 6B_1–B_3). In the fibula, longitudinal vascular canals are still the main type of vascular organization (Fig. 6D). The quantity of circular vascular canals also increases dramatically, when compared to the juvenile stage (Fig. 6). There are no longitudinal vascular canals in radial rows developing in this ontogenetic stage, which is different from the previous two stages.

Vascularization is slightly reduced in the outer cortex, compared to the inner cortex, and densities of vascular canals are much lower (31 per field of view; 127 per mm^2) than in hatchling (46 per field of view; 189 per mm^2) and juvenile (40 per field of view; 164 per mm^2) stages (SOM: table S7). The main bone tissue is fibrolamellar bone, but there are parallel-fibred bone deposits in the outermost cortex which is distinguished from that in the juvenile stage (Fig. 6). Secondary osteons are present in the deeper cortex (Fig. 6E). Most osteocyte lacunae are flattened in cross section in the outer cortex, but oval in the inner cortex. The fibula has endosteal bone around the medullary cavity, while several large erosion cavities are present in the remodelling zone.

Much lamellar bone also can be observed around the LAGs. Endosteal bone in the fibula (Fig. 6E) developed much better than other bones (Fig. 6F–G). Erosion cavities around the medullary cavity develops quite well in the radius and femur (Fig. 6F), but less developed in the tibia (Fig. 6E, G).

Adult stage.—We identify IVPP V18343 and IVPP V12617 as the adult, or near-adult, specimens, based on bone histology characters and the fact that they have eight LAGs and the estimated age is over ten years old. We took thin sections from the right humerus (Fig. 7A, B), radius (Fig. 7C), tibia (Fig. 7D, E) and fibula (Fig. 7F).

Longitudinal vascular canals dominate the thin section of the right tibia, humerus, and radius. Eight LAGs were observed in the cortex of the tibia, but still no EFS (Horner et al. 1999), indicating that the bone is not from a fully-growth

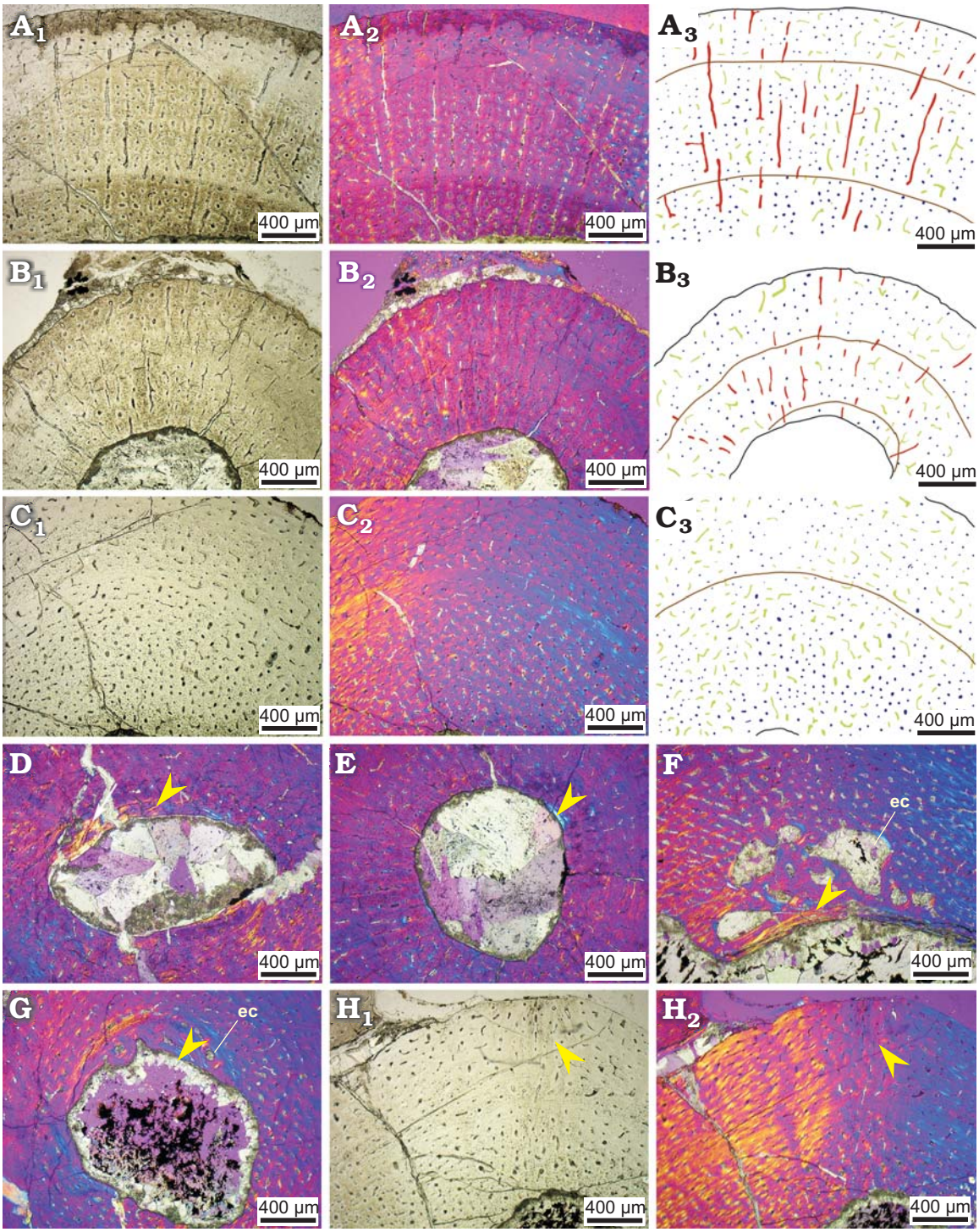

Fig. 4. Bone microstructure in juvenile ceratopsian dinosaur *Psittacosaurus lujiatunensis* Zhou, Gao, Fox, and Chen, 2006 from western Liaoning, China, Early Cretaceous. Mid-diaphyseal transverse section of right humerus (IVPP V14341.1, **A**), right radius (IVPP V14341.6, **B**), left tibia (IVPP V14341.5, **C**). Endosteal bone (arrow) showing in the inner most cortex and medullary cavity of right ulna (IVPP V14341.6, **D**), right radius (IVPP V14341.6, **E**), right femur (IVPP V14341.1, **F**), right fibula (IVPP V14341.1, **G**). Sharpey's fibres (arrows) in left tibia (IVPP V14341.5, **H**). Photographs in regular transmitted light (A_1–C_1, H_1), elliptically polarized light (A_2–C_2, D, E, F, G, H_2), line drawings (A_3–C_3) showing longitudinal vascular canals (navy), reticular vascular canals (green), radial vascular canals (red), and LAGs (brown lines). Abbreviation: ec, erosion cavity.

adult. Triple LAGs were present in the outer cortex in all three bones in IVPP V12617, and the thick parallel-fibred bone with less vascularization in the outer cortex. All these features show that IVPP V12617 grew very slowly and is close to fully-grown. Fibrolamellar bone is still the main bone tissue in the middle cortex.

The density of vascular canals in the outer cortex is much lower than in earlier growth stages, being only 12 per field of

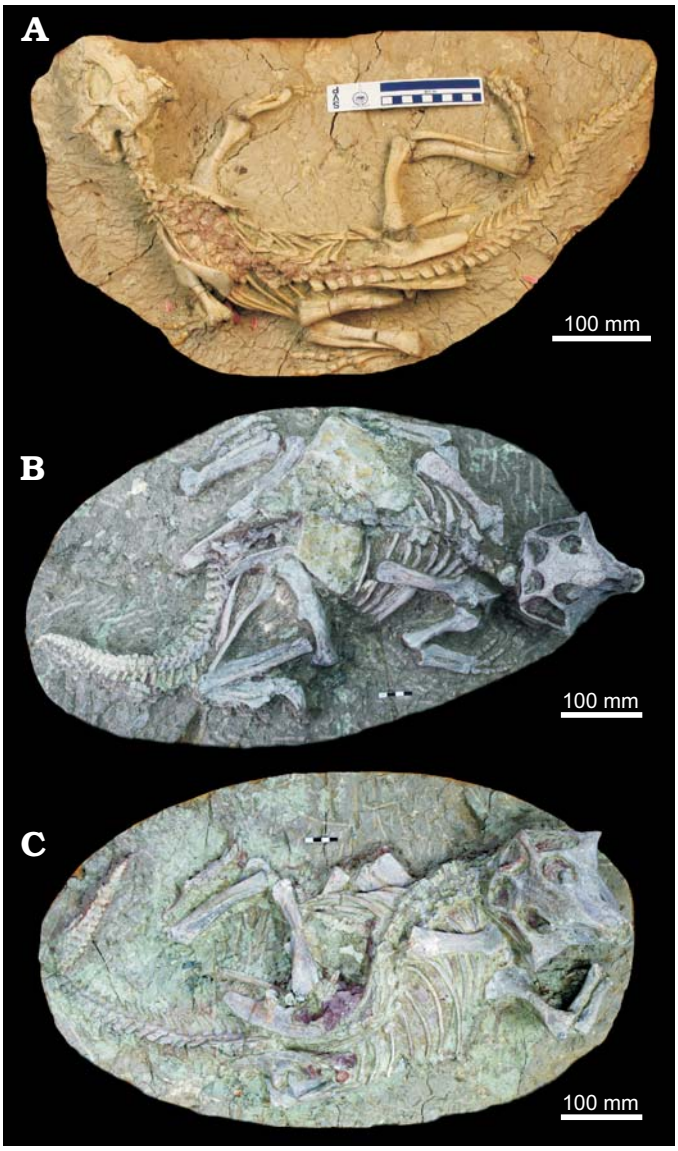

Fig. 5. The skeletons of ceratopsian dinosaur *Psittacosaurus lujiatunensis* Zhou, Gao, Fox, and Chen, 2006 subadult (IVPP V14748, **A**; IVPP V18344, **B**) and adult *P. lujiatunensis* (IVPP V18343, **C**) from western Liaoning, China, Early Cretaceous.

view (49 per mm^2; SOM: table S7), which also means that the growth rate had become very slow. The density of osteocyte lacunae does not differ significantly from the previous ontogenetic stages. Although primary osteons are still the main type of osteons in the cortex, more secondary osteons are present in the inner cortex in this adult stage. Remodelling of secondary osteons occurs in the innermost cortex around the thick endosteal bone (Fig. 7E). All the bones have endosteal bone deposited around the medullary cavity, and it is especially thick in the tibia (Fig. 7E). The erosion cavities are very well developed in all bones, especially in the humerus, and they reach to the middle cortex (Fig. 7B).

Vascular canal organization in the radius is different from that in the other bones. In the middle cortex of the radius, there are some radial vascular canals (Fig. 7C), which are consistent with observations in the juvenile stage.

Discussion

Bone histology differs through the ontogeny.—The dominant bone tissue is fibrolamellar bone in the long bones of *P. lujiatunensis* of four ontogenetic stages that we recognized (Table 2), but it shows variations among different stages. The changing density of vascular canals in the outer cortex through the growth stages (SOM: table S7, 189–164–127–49 per mm^2) and the shape of the osteocyte lacunae, suggests that *P. lujiatunensis* grew faster in early stages (hatchling, juvenile, and subadult). But the density of vascular canals in the outermost cortex of the tibia decreases slightly and the parallel-fibred bone appears in the periosteal surface in the subadult stage, which means that the growth rate was slowing down at this ontogenetic stage. The low density of vascular canals in the outmost cortex shows that the growth rate decreases dramatically in the adult stage.

Through the ontogenetic changes in bone histology, we found that simple primary vascular canals were deposited in the outer cortex in the hatchling and juvenile, and are also present in subadult and adult stages. Secondary osteons only occur in subadults and adults, although primary osteons are the dominant system throughout life. Bone remodelling associated with secondary osteons is present close to the endosteal bone in the adult stage. Longitudinal vascular canals in radial rows are obvious in hatchling and juvenile stages. Circular primary osteons are absent in the hatchling stage, rare in juvenile and adult stages, and abundant in the sub-adult stage. Parallel-fibred bones in the outer cortex are just seen in the sub-adult and adult and become thicker with age. Endosteal bone is absent in the hatchling stage, incomplete and thin in juveniles, complete and thin in the fibula in subadults, and complete and thick in adults. Erosion cavities are absent in the hatchling stage, developing in the femur and fibula in the juvenile stage, increasing in the subadult stage, and abundant in the adult stage. Even in a single skeleton, different bones may show slightly different ontogenetic stages; for example, we confirm that the fibula may appear to be from an older animal, having more LAGs in some cases, than the other limb elements. This makes it harder to divide the growth sequence into too many stages, and we use only four stages here, and summarize the differences between elements under each of those four growth stages.

We have stressed here the need to consider multiple bones from a single individual to ensure some control on matching the number of LAGs to the age of the individual. Similarly, Horner et al. (1999) noticed that in a single skeleton of an individual dinosaur different bones may display different numbers of "growth rings" (= LAGs). This is probably because different bones in the skeleton have different morphology, and each follows specific remodelling processes, as noted also from studies of modern alligator bone histology (Woodward et al. 2014). For example, a neural spine grows differently from a tibia (Chinsamy-Turan 2005), and in *Hypacrosaurus stebingeri* long bones, the tibia and the femur have eight growth rings, while the radius and

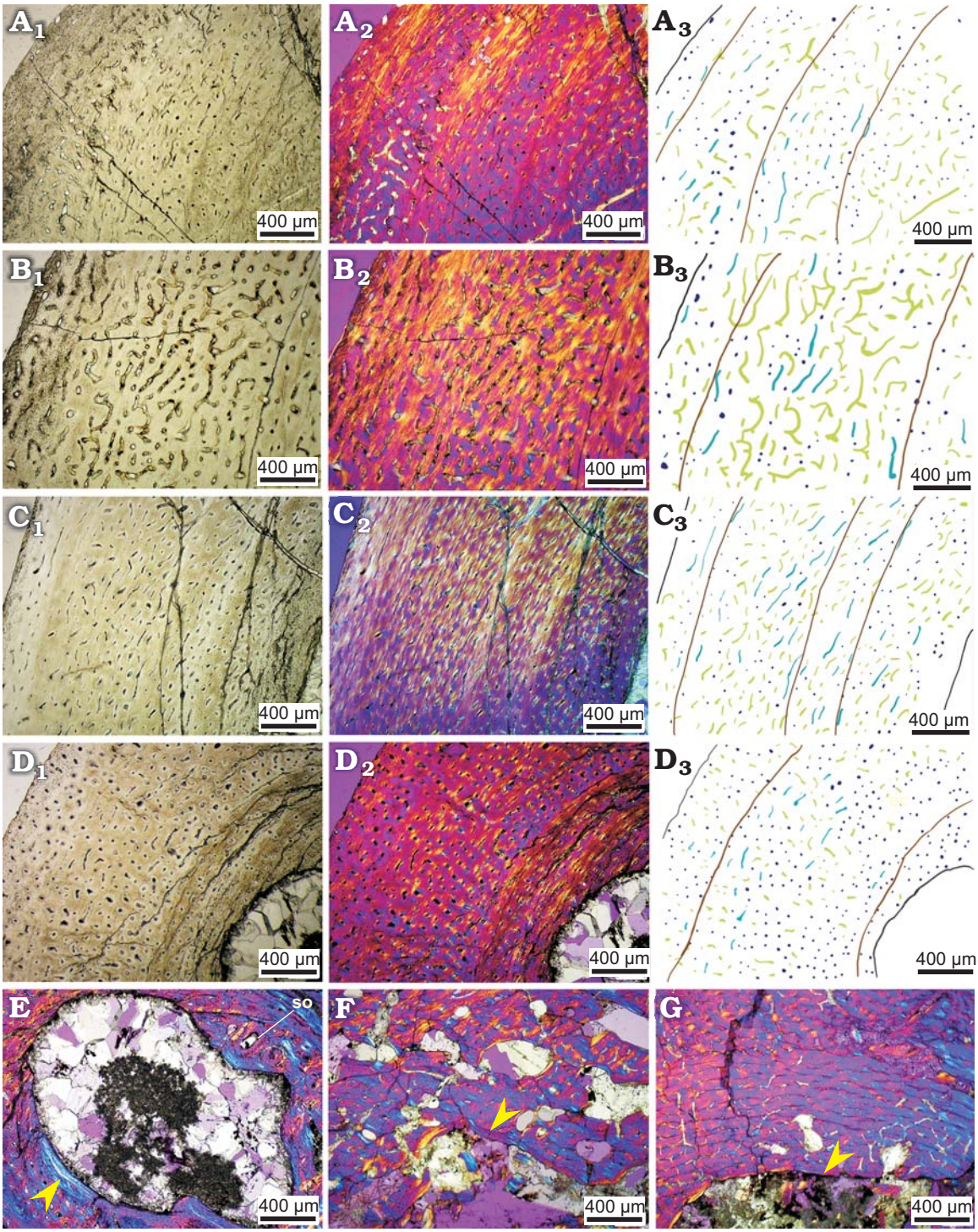

Fig. 6. Bone microstructure in subadult ceratopsian dinosaur *Psittacosaurus lujiatunensis* Zhou, Gao, Fox, and Chen, 2006 from western Liaoning, China, Early Cretaceous. Mid-diaphyseal transverse section of right radius (IVPP V18344, **A**), left femur (IVPP V18344, **B**), left tibia (IVPP V14748, **C**), left fibula (IVPP V14748, **D**, **E**), left femur (IVPP 18344, **F**), left tibia (IVPP V18344, **G**). E–G show the endosteal bone (arrows). Photographs in regular transmitted light (A_1–D_1), elliptically polarized light (A_2–D_2, E–G); line drawings (A_3–C_3) showing longitudinal vascular canals (navy), reticular vascular canals (green), radial vascular canals (red), and LAGs (brown lines). Abbreviation: so, secondary osteons.

fibula have just seven growth rings (Horner et al. 1999). We found a similar kind of variation in *Psittacosaurus lujiatunensis*, in the different numbers of growth rings in different long bones in IVPP V 14341.1, with two LAGs in the right tibia and three LAGs in the right femur and right humerus.

Two *Psittacosaurus* species show different ontogenetic patterns of bone histology.—The histological patterns observed in this study differ in some respects from those previously reported in a growth series of *Psittacosaurus mongoliensis* from the Lower Cretaceous of Mongolia sampled

by Erickson and Tumanova (2000). The key differences are: (i) Medullary cavity expansion affects the earliest formed bone in each element no later than age 6 in *P. mongoliensis*, but happened much earlier (age 3 in tibia) in *P. lujiatunensis*. (ii) The presence of endosteal bone in *P. mongoliensis* varies and shows no relationship to growth stage, but in *P. lujiatunensis*, endosteal bone shows very clear ontogenetic development. (iii) The tibial diaphysis of neonate *P. mongoliensis* primarily showed longitudinal vascular canals and fewer reticular vascular canals, whereas in *P. lujiatunensis*, the dominant vascular canals are reticular vascular canals, but this may be caused by using different approaches which we mentioned before. (iv) The tibia of *P. mongoliensis* in its eighth year shows abundant radially oriented vascular canals near the periosteal surface, which is very similar to the pathologic bone tissue showed in a Transylvanian dinosaur (Chinsamy and Tumarkin-Deratzian 2009), but in *P. lujiatunensis*, most radial vascular canals were present in the forelimbs at a younger age, which indicates differential relative growth of forelimb and hindlimb (Zhao et al. 2013). (v) The dominant vascularization in the adult stage is reticular in *P. mongoliensis*, but longitudinal in *P. lujiatunensis*. (vi) Erosion cavities are present much earlier in *P. lujiatunensis* (age 3 in femur and fibula) than *P. mongoliensis* (age 8).

The largest hindlimb bones (femur and tibia) in the *Psittacosaurus mongoliensis* growth series, representing individuals up to nine years old, show that radially vascularized fibrolamellar bone was deposited along part of the mid-shaft circumference beginning at the age of seven. Other parts of the mid-shaft circumference have only reticular or even longitudinal vascularization. This indicates that the local apposition rate differed greatly along the circumference of the bone, presumably reflecting osseous drift (Erickson and Tumanova 2000; Erickson et al. 2009), which is also the case in *P. lujiatunensis*. The fitted growth curve for *P. mongoliensis* (Erickson and Tumanova 2000: fig. 4) indicates that at age 9 the largest sampled individuals had reached perhaps 80% of final body mass, a conclusion consistent with the lack of an EFS in any of the sampled bones.

The largest histologically sampled individuals of *P. mongoliensis* thus appear to have been well short of their final adult size and still within the exponential phase of growth (Erickson and Tumanova 2000), perhaps indicating that the presence of radial canals in the hindlimb bones simply reflects normal growth along a sigmoid curve of mass vs. age, as in other dinosaurs including *P. lujiatunensis* (Erickson et al. 2009; Padian and Lamm 2013). However, the fact that the radial canals are limited to the hindlimb might suggest fast growth of the hindlimb relative to the forelimb at this stage of ontogeny (Francillon-Vieillot et al. 1990; de Margerie et al. 2004; Padian and Lamm 2013), perhaps indicating a quadrupedal-to-bipedal postural shift like that inferred for *P. lujiatunensis* (Zhao et al. 2013). However, dense radial vascular canals were not observed in any of the hindlimb bones that we sectioned, suggesting that their occurrence in *P. mongoliensis* is a result of pathology (Chinsamy and Tumarkin-Deratzian 2009). The largest *P. mongoliensis* femur sampled was 210 mm long, representing a nine-year-old animal that had still not reached maximal body size, as mentioned above. By contrast, the largest known *P. lujiatunensis* femur measures 202 mm (Erickson et al. 2009) and must have been close to final size because the largest femur sampled in the present study is only about 160 mm long but appears almost fully grown on the basis of histology. This femur represents an individual (IVPP V12617) that we consider to be ten years old on the basis of histology, although it was previously interpreted as a six-year-old on the basis of femur size alone (Erickson et al. 2009). This finding helps support the conclusions of Woodward et al. (2015), who argued that age cannot be accurately determined from element length due to individual variation in growth rates.

Growth curves.—Erickson and Tumanova (2000) and Erickson et al. (2009) calculated growth curves for the two species of *Psittacosaurus* using evidence of overall body size change and counts of LAGs. Their work was heavily criticised by Myhrvold (2013, 2015), who argued that this earlier work could be seen as heavily compromised or incorrect. However, Erickson et al. (2015) responded robustly, explained differences in approach and misunderstandings, and provided detailed documentation of what they did. The original growth curve for *P. lujiatunensis* provided by Erickson et al. (2009) has been corrected (Erickson et al. 2009: fig. 6, corrigendum; 2015), and it confirms sexual maturity of *P. lujiatunensis* no later than ten years old, as indicated in the original paper.

In our case, femur length comparisons informed by histology suggest larger adult body size in *P. mongoliensis*, but inferred growth curves for the two species (Erickson and Tumanova 2000; Erickson et al. 2009) show a considerably higher mass for *P. lujiatunensis* than for *P. mongoliensis* (38 and 25 kg, respectively). There are several possible solutions to this observation, including comparing the mass estimates used to construct growth curves based on circumference as well as length measurements (Erickson and Tumanova 2000; Erickson et al. 2009), but it can only be solved by an analysis directly comparing the two species in terms of both histology and skeletal proportions. We note, however, that both logistic growth curves extrapolate beyond the available histological data, and we therefore prefer the direct histological and meristic evidence suggesting that *P. mongoliensis* grew to a larger final size than *P. lujiatunensis*.

Fig. 7. Bone microstructure in subadult ceratopsian dinosaur *Psittacosaurus lujiatunensis* Zhou, Gao, Fox, and Chen, 2006 from western Liaoning, China, Early Cretaceous. The outer cortex of mid-diaphyseal transverse section of right humerus (IVPP V12617, **A**), right radius (IVPP V12617, **C**), right tibia (IVPP V12617, **D**). The inner most cortex of mid-diaphyseal transverse section of right humerus (IVPP V12617, **B**), right tibia (IVPP V12617, **E**). Mid-diaphyseal transverse section of fibula (IVPP V18343, **F**). Photographs in regular transmitted light (A_1–F_1), elliptically polarized light (A_2–F_2), crossed plane-polarized light (B_3, E_3); line drawings (A_3, C_3, D_3, F_3) showing longitudinal vascular canals (navy), reticular vascular canals (green), radial vascular canals (red), and LAGs (brown lines). →

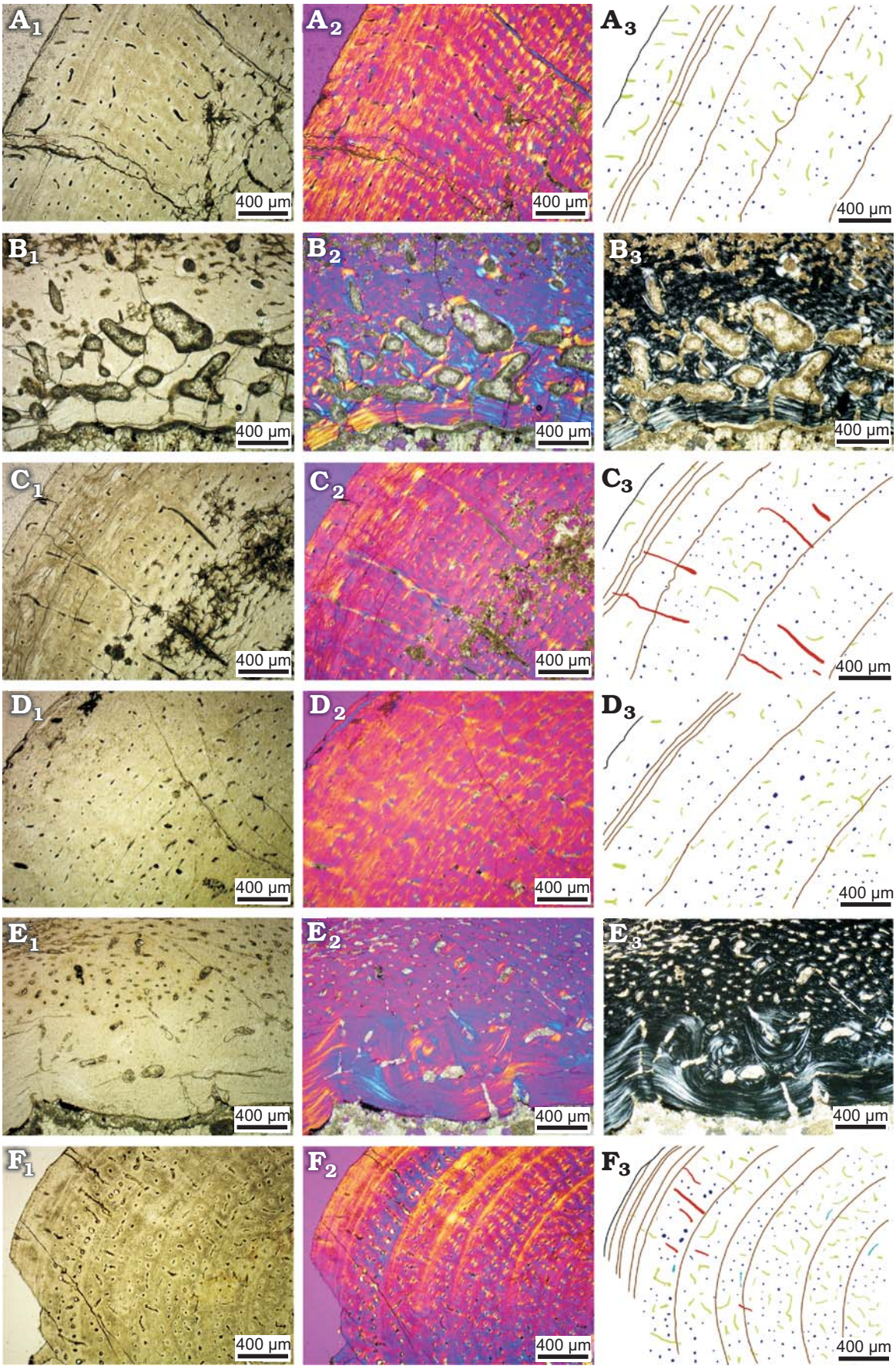
A1
400 μm
A2
400 μm
A3
400 μm
B1
400 μm
B2
400 μm
B3
400 μm
C1
400 μm
C2
400 μm
C3
400 μm
D1
400 μm
D2
400 μm
D3
400 μm
E1
400 μm
E2
400 μm
E3
400 μm
F1
400 μm
F2
400 μm
F3
400 μm

Conclusions

Our study shows that bone histology in the Early Cretaceous ceratopsian dinosaur *Psittacosaurus lujiatunensis* Zhou, Gao, Fox, and Chen, 2006 varied through growth. The dominant bone type is fibrolamellar throughout (except the hatchling stage), but vascular canal density reduces sharply from 189 to 49 per mm^2 from hatchling to adult. This occurrence and the completion of endosteal bone confirms that growth was fastest in the early stages, slowing in the subadult to adult stage. We note differences in bone histology and LAG count between different bones from the same individuals. We find some differences in bone histology during growth when compared to the related species *P. mongoliensis* Osborn, 1923, which probably grew to a larger final adult size.

Acknowledgements

We thank P. Martin Sander (University of Bonn, Germany) for helping and training in bone histology, and Shukang Zhang and Zichuan Qin (both IVPP) for helping in thin section preparation. We thank Holly Woodward (Oklahoma State University, Stillwater, USA) and Michael D'Emic (Adelphi University, Garden City, USA) for their very helpful comments on the MS in review. This study was supported by grants from the National Natural Science Foundation of China (41502018 and 41688103), the Youth Innovation Promotion Association of Chinese Academy of Sciences (2015057), Newton Advanced Fellowships of Royal Society (NA160290), and the Strategic Priority Research Program of Chinese Academy of Sciences (XDB26000000, XDB183030504).

References

An, Y.H. and Martin, K.L. 2003. *Handbook of Histology Methods for Bone and Cartilage*. 588 pp. Springer Science & Business Media, New York.

Castanet, J. 2006. Time recording in bone microstructures of endothermic animals; functional relationships. *Comptes Rendus Palevol* 5: 629–636.

Castanet, J., Francillon-Vieillot, H., Meunier, F.J., and Ricqlès, A. de 1993. Bone and individual aging. *In*: B.K. Hall (ed.), *Bone. Volume 7: Bone growth B*, 245–283. CRC Press, Boca Raton.

Chinsamy, A. and Tumarkin-Deratzian, A. 2009. Pathologic bone tissues in a Turkey vulture and a nonavian dinosaur: implications for interpreting endosteal bone and radial fibrolamellar bone in fossil dinosaurs. *The Anatomical Record* 292: 1478–1484.

Chinsamy-Turan, A. 2005. *The Microstructure of Dinosaur Bone: Deciphering Biology with Fine-scale Techniques*. 195 pp. The Johns Hopkins University Press, Baltimore.

de Margerie, E., Robin, J.-P., Verrier, D., Cubo, J., Groscolas, R., and Castanet, J. 2004. Assessing a relationship between bone microstructure and growth rate: a fluorescent labelling study in the king penguin chick (*Aptenodytes patagonicus*). *Journal of Experimental Biology* 207: 869–879.

Erickson, G.M. 2005. Assessing dinosaur growth patterns: a microscopic revolution. *Trends in Ecology & Evolution* 20: 677–684.

Erickson, G.M. and Tumanova, T.A. 2000. Growth curve of *Psittacosaurus mongoliensis* Osborn (Ceratopsia: Psittacosauridae) inferred from long bone histology. *Zoological Journal of the Linnean Society* 130: 551–566.

Erickson, G.M., Currie, P.J., Inouye, B.D., and Winn, A.A. 2006. Tyrannosaur life tables: An example of nonavian dinosaur population biology. *Science* 313: 213–217.

Erickson, G.M., Makovicky, P. J., Currie, P. J., Norell, M.A., Yerby, S.A., and Brochu, C.A. 2004. Gigantism and comparative life-history parameters of tyrannosaurid dinosaurs. *Nature* 430: 772–775.

Erickson, G.M., Makovicky, P.J., Inouye, B.D., Zhou, C.F., and Gao, K.Q. 2009. A life table for *Psittacosaurus lujiatunensis*: initial insights into ornithischian dinosaur population biology. *The Anatomical Record* 292: 1514–1521.

Erickson, G.M., Makovicky, P.J., Inouye, B.D., Zhou, C.F., and Gao, K.Q. 2015. Flawed analysis? A response to Myrhvold. *The Anatomical Record* 298: 1669–1672

Erickson, G.M., Rogers, K.C., Varrichio, D.J., Norell, M.A., and Xu, X. 2007. Growth patterns in brooding dinosaurs reveals the timing of sexual maturity in non-avian dinosaurs and genesis of the avian condition. *Biology Letters* 3: 558–561.

Erickson, G.M., Rogers, K.C., and Yerby, S.A. 2001. Dinosaurian growth patterns and rapid avian growth rates. *Nature* 412: 429–433.

Francillon-Vieillot, H., Buffrénil, V. de, Castanet, J., Géraudie, J., Meunier, F.J., Sire, J.Y., Zylberberg, L., and Ricqlès, A. de 1990. Microstructure and mineralization of vertebrate skeletal tissues. *In*: J.G. Carter (ed.), *Skeletal Biomineralization: Patterns, Processes and Evolutionary Trends. Vol. 1*, 471–530. Van Nostrand Reinhold, New York.

Horner, J.R., Ricqlès, A. de, and Padian, K. 1999. Variation in dinosaur skeletochronology indicators: implications for age assessment and physiology. *Paleobiology* 25: 295–304.

Horner, J.R., Ricqlès, A. de, and Padian, K. 2000. Long bone histology of the hadrosaurid dinosaur *Maiasaura peeblesorum*: Growth dynamics and physiology based on an ontogenetic series of skeletal elements. *Journal of Vertebrate Paleontology* 20: 115–129.

Kerp, H. and Bomfleur, B. 2011. Photography of plant fossils—new techniques, old tricks. *Review of Palaeobotany & Palynology* 166: 117–151.

Klein, N. and Sander, M. 2008. Ontogenetic stages in the long bone histology of sauropod dinosaurs. *Paleobiology* 34: 247–263.

Klein, N., Sander, M., and Suteethorn, V. 2009. Bone histology and its implications for the life history and growth of the Early Cretaceous titanosaur *Phuwiangosaurus sirindhornae*. *Geological Society, London, Special Publications* 315: 217–228.

Köhler, M., Marin-Mortalla, N., Jordana, X., and Aanes, R. 2012. Seasonal bone growth and physiology in endotherms shed light on dinosaur physiology. *Nature* 487: 358–361.

Myhrvold, N.P. 2013. Revisiting the estimation of dinosaur growth rates. *PLoS One* 8 : e81917.

Myhrvold, N.P. 2015. Problems in Erickson et al. 2009. *The Anatomical Record* 298: 489–493.

Padian, K. and Lamm, W. 2013. *Bone Histology of Fossil Tetrapods: Advancing Methods, Analysis, and Interpretation*. 285 pp. University of California Press, Berkeley.

Ricqlès, A. de, Meunier, F.J., Castanet, J., and Francillon-Vieillot, H. 1991. Comparative microstructure of bone. *In*: B.K. Hall (ed.), *Bone. Vol. 3: Bone Matrix and Bone Specific Products*, 1–78. CRC Press, Boca Raton.

Sander, P. M. 2000. Longbone histology of the Tendaguru sauropods: implications for growth and biology. *Paleobiology* 26: 466–488.

Sander, P. M. and Klein, N. 2005. Developmental plasticity in the life history of a prosauropod dinosaur. *Science* 310: 1800–1802.

Sander P. M., Klein, N., Buffetaut, E., Cuny, G., Suteethorn, V., and Le Loeuff, J. 2004. Adaptive radiation in sauropod dinosaurs: bone histology indicates rapid evolution of giant body size through acceleration. *Organisms Diversity & Evolution* 4: 165–173.

Selden, P.A. and Penney, D. 2017. Imaging techniques in the study of fossil spiders. *Earth-Science Reviews* 166: 111–131.

Wang, S., Zhang, S.K., Sullivan, C., and Xu, X. 2016. Elongatoolithid eggs containing oviraptorid (Theropoda, Oviraptorosauria) embryos from the Upper Cretaceous of Southern China. *BMC Evolutionary Biology* 16: 67.

Woodward, H. N., Freedman Fowler, E.A., Farlow, J.O., and Horner, J.R. 2015. *Maiasaura*, a model organism for extinct vertebrate population biology: a large sample statistical assessment of growth dynamics and survivorship. *Paleobiology* 41: 503–527.

Woodward, H.N., Horner, J.R., and Farlow, J.O. 2014. Quantification of intraskeletal histovariability in *Alligator mississippiensis* and implications for vertebrate osteohistology. *PeerJ* 2: e422.

Zhao, Q., Benton, M.J., Sullivan, C., Sander, M.P., and Xu, X. 2013. Histology and postural change during the growth of the ceratopsian dinosaur *Psittacosaurus lujiatunensis*. *Nature Communications* 4: 2079.